Use of ultrafast-laser-driven microexplosion for fabricating three-dimensional void-based diamond-lattice photonic crystals in a solid polymer material

Guangyong Zhou, Michael James Ventura, Michael Ross Vanner, and Min Gu

Centre for Micro-Photonics and Centre for Ultra-high Bandwidth Devices for Optical Systems, School of Biophysical Sciences and Electrical Engineering, Swinburne University of Technology, P.O. Box 218, Hawthorn, Victoria 3122, Australia

Received May 26, 2004

Micro-sized void spheres are successfully generated in a solid polymer by use of a tightly focused femtosecond laser beam from a high-repetition-rate laser oscillator. Confocal reflection images show that the void spheres are longitudinal rotational symmetric ellipsoids with a ratio of long to short axes of approximately 1.5. Layers of void spheres are then stacked to create three-dimensional diamond-lattice photonic crystals. Three gaps are observed in the [100] direction with a suppression rate of the second gap of up to approximately 75% for a 32-layer structure. The observed first- and second-order gaps shift to longer and shorter wavelengths, respectively, as the angle of incidence increases. © 2004 Optical Society of America

OCIS codes: 220.4000, 160.5470, 160.4760, 300.6340, 140.7090.

In recent years the fabrication of photonic crystals has attracted extensive interest because such artificial periodic structures can control the behavior of light in the way that semiconductors control the behavior of electrons.[1,2] One of the most important goals in photonic bandgap technology is the search for methods to produce three-dimensional (3D) lattices with a complete photonic bandgap (CPBG) in the optical spectral regions. In general, structures with a more spherical Brillouin zone, such as face-centered-cubic (fcc) and diamond lattices, are more likely to open 3D photonic bandgaps.[3] A diamond lattice fares much better than a fcc lattice for the following reasons: First, the threshold value of the refractive-index contrast to open a CPBG is approximately 2 for a diamond lattice rather than 2.8 for a fcc lattice.[4,5] Second, a CPBG appears between the second and the third bands for a diamond lattice rather than between the eighth and the ninth bands for a fcc lattice,[6] which is therefore much more stable against disorders and defects.[7,8] Third, the bandgap is significantly larger for a diamond lattice.[3] In addition, according to the calculation,[3] diamond photonic crystals with air spheres in a dielectric matrix can open a larger gap compared with those with dielectric spheres in the air matrix. Until now, the fabrication of 3D photonic crystals with air spheres remained a big challenge. Inverse fcc opal lattices consisting of air spheres can be fabricated by templating of self-assembled latex colloids with high refractive-index materials.[9,10] Opallike diamond structures were also fabricated by use of the robot-aided micromanipulation templating method.[11] But the templating method is complicated and time consuming and can produce many uncontrollable defects.

Ultrafast-laser-driven microexplosion was used to generate void spheres in some solid transparent materials.[12–16] The material is ejected from the focal point. This process forms a void sphere surrounded by a region of compacted material. This technique is a one-step approach that does not require chemical post-processing and results in high-quality void spheres. This method has been used in multilayer read-only bit optical data storage.[15,16] In this Letter we apply this method to fabricate 3D diamond photonic crystals with air spheres in a solid polymer material. The photonic bandgap properties are studied, and the bandgap measurement method is discussed.

The experimental setup we used is similar to that used in Refs. 17–19. A 740-nm femtosecond laser beam from a Tsunami femtosecond laser (Spectra-Physics, Mountainview, Calif.) was tightly focused into a polymerized resin [Norland Optical Adhesive (NOA) 63, Norland Products, Inc., Cranbury, N.J.] through an Olympus 60×, 1.45-numerical-aperture oil-immersion objective. Figure 1(a) schematically shows the unit cell of the diamond lattice. Fabricated void spheres as well as diamond photonic crystals were examined by use of confocal reflection microscopy (Fluoview, Olympus, Japan). Figure 1(b) shows the $x-y$ confocal reflection (left) and transmission (right) microscope images of a single void sphere that was generated 10 μm below the top surface of the polymer film with a laser power of 60 mW and an exposure time of 10 ms. The lateral diameter of the void sphere is approximately 1.7 μm. Figure 1(c) shows the $x-z$ scanning confocal reflection (left) and transmission image (right) of the same void sphere. Two bright spots in the confocal reflection image represent the strong reflection from the top and bottom surfaces of the void sphere with a distance of approximately 2.5 μm, which indicates the longitudinal size of the void cavity. Therefore the fabricated void sphere is a longitudinal rotational symmetric ellipsoid with a ratio of long to short axes of approximately 1.5. Figure 1(d) shows the dependence of the lateral diameter of the void sphere as a function of exposure time at two different laser powers. Increasing the power or exposure time causes the diameter of the void spheres to increase correspondingly. All photonic crystals reported in this Letter were fabricated with

0146-9592/04/192240-03$15.00/0

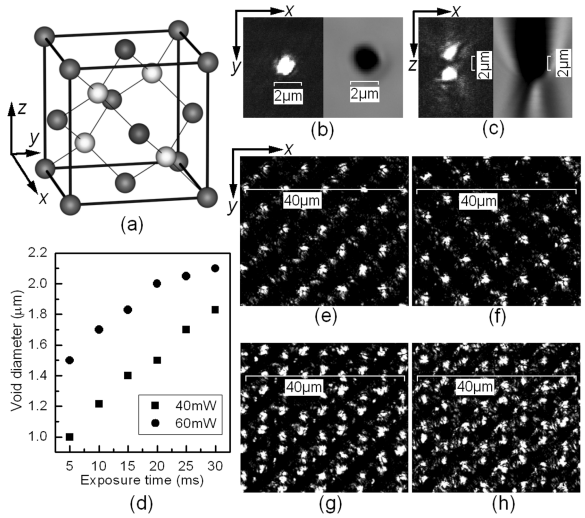

Fig. 1. (a) Illustration of the diamond lattices, (b) confocal reflection (left) and transmission (right) microscope images, (c) $x-z$ scanning confocal reflection (left) and transmission (right) microscope images of one void, (d) void diameter as a function of exposure time at powers of 40 and 60 mW, (e), (f) confocal reflection images of the top four layers of the diamond lattice structure in the [100] direction ($a = 10\ \mu$m).

a laser power of 40 mW and an exposure time of 10 ms.

Figures 1(e)–1(h) show the $x-y$ confocal reflection images of the top four layers of void spheres of a 3D diamond photonic crystal stacked in the [100] direction with a lattice constant of $a = 10\ \mu$m. The layer spacing is $a/4$. The scale bars generated by the confocal microscope control program are used as a reference. A diamond lattice with a layer periodicity of 4 is composed of two sets of fcc lattices offset by $a/4$ in the x, y, and z directions relative to each other. From Figs. 1(e) and 1(f) one can see that there is an $a/4$ shift in the x and y directions for the second layer compared with the first layer. Figure 1(g) indicates an $a/4$ shift of the third layer compared with the first layer. Figure 1(h) indicates an $a/4$ shift of the fourth layer compared with the third layer. Because of the strong scattering from the top several layers, confocal reflection images for deeper layers cannot be obtained.[17]

The best way to check the uniformity of the void sphere lattices is to measure the transmission spectra of the fabricated structures. A Nicolet Nexus Fourier transform infrared spectrometer was used to provide infrared light with a wavelength from 1 to 5 μm and a 32×, 0.65-numerical-aperture reflective objective (Reflechromat, Thermo Nicolet, Madison, Wisc.) was used to focus the light beam on the structure. However, no bandgap can be observed with the objective as it is. The reason is that the reflective objective provides an incident hollow light cone with an outer angle of 40° and an inner angle of 15° (which corresponds to 25° and 10° in the sample). The measured spectrum is the average result over the incident angle range. To reduce the range of the angle of incidence, an off-center aperture corresponding to a half-angle of 5° was attached to the Fourier transform infrared objective. By adjusting the position of the aperture and tilting the sample, we achieved illumination at different angles of incidence. The transmission spectrum with a 3° average angle of incidence is shown in Fig. 2, revealing strong suppression peaks. The strong suppression rate of the observed first- and second-order gaps, approximately 65% and 75%, respectively, indicates that the fabricated void spheres are well correlated with each other.

The photonic bandgap properties of 3D diamond-lattice photonic crystals depend on the lattice direction. Therefore the angle dependence of the bandgap properties of a 3D diamond structure stacked in the [100] direction with lattice constants of 4.44 μm was investigated. Figure 2 shows the baseline-corrected transmission spectra of different angles of incidence. The observed first-order gap shifts to a longer wavelength, whereas the observed second-order gap shifts to a shorter wavelength when the angle of incidence increases. The midgap wavelength as a function of the angle of incidence of the first- and second-order

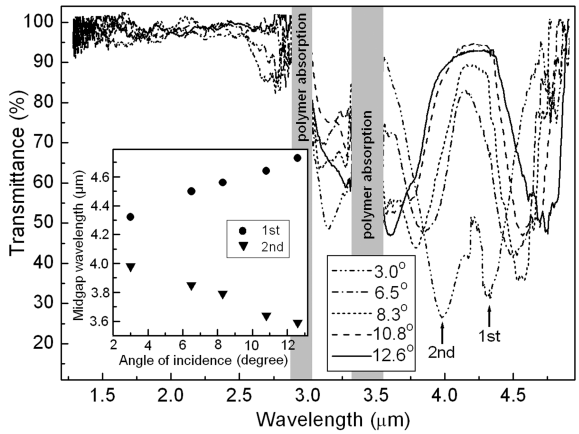

Fig. 2. Baseline-corrected transmission spectra of 3D diamond photonic crystals stacked in the [100] direction ($a = 4.44\ \mu$m) at different directions of light incidence. The dependence of the midgap wavelength on the angle of incidence is given in the inset.

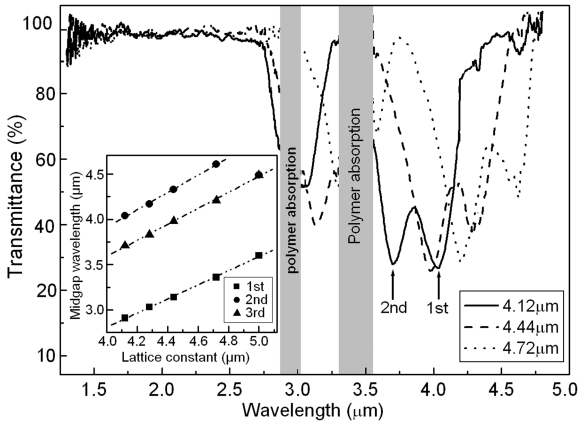

Fig. 3. Baseline-corrected transmission spectra of 3D void diamond photonic crystals stacked in the [100] direction with lattice constants of 4.12, 4.44, and 4.72 μm. Inset, midgap wavelength of the three observed gaps as a function of the lattice constant.

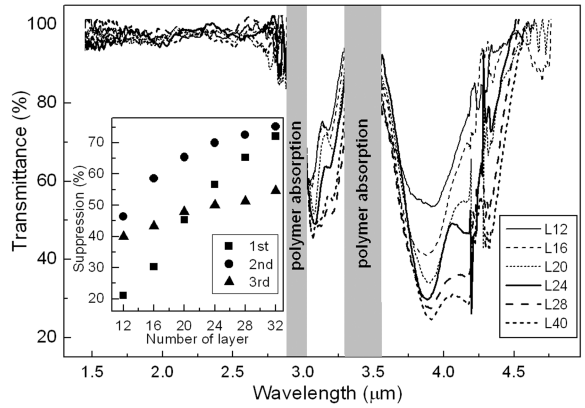

Fig. 4. Baseline-corrected transmission spectra of 3D diamond void photonic crystals stacked in the [100] direction ($a = 4.28\ \mu$m) for different numbers of layers. The midgap wavelength of the observed first-, second-, and third-order gaps as a function of the layer number is plotted in the inset. Labels L12, ..., L32 denote the layer numbers 12, ..., 32, respectively.

gaps is shown in the inset of Fig. 2. It is expected that the observed first- and second-order gaps would overlap in the [100] direction. The sensitive angle dependence of the bandgap can explain why no bandgap is observed without the use of a small aperture.

To confirm that the wavelength of the bandgap should be in proportion with the lattice constant, diamond structures with various lattice constants were fabricated along the [100] direction. Figure 3 shows the baseline-corrected transmission spectra of 32-layer 3D diamond void photonic crystals stacked in the [100] direction with lattice constants of 4.12, 4.44, and 4.72 μm, respectively. All the gaps shift to longer wavelengths as the lattice constant increases. The inset shows the dependence of the midgap wavelength for the three observed gaps as a function of lattice constant. As expected, a linear relationship is observed.

Finally, the dependence of the suppression rate of the observed gaps on the layer number was studied. Figure 4 shows the baseline-corrected transmission spectra of the photonic crystals consisting of different layers of void spheres with a lattice constant of 4.28 μm. The transmittance of the three observed gaps as a function of the layer numbers is shown in the inset. Increasing the layer number from 12 to 32, the suppression rate increases from 46% to 75% for the observed second-order gap.

As is well known, focal point aberration exists if the refractive index of the sample does not match that of the immersion medium; the larger the mismatching, the stronger the aberration.[20] Because the refractive index of solidified NOA 63 resin ($n = 1.56$) is close to that of the immersion oil (1.52), the focal point aberration is not pronounced and therefore does not affect the fabrication of photonic crystals severely.

In conclusion, longitudinal rotational symmetric ellipsoidal void spheres with a ratio of long to short axes of approximately 1.5 have been fabricated in a solid NOA 63 resin by use of a tightly focused ultrafast laser beam from a high-repetition-rate laser oscillator. A characterization based on confocal reflection microscopy indicates that such void spheres can be stacked into well-correlated diamond-lattice structures. The 3D diamond-lattice photonic crystals stacked in the [100] direction show three gaps with strong suppression. The angle dependence of the bandgap properties reveals that the observed first-order gap shifts to the longer wavelength, whereas the second-order gap shifts to the shorter wavelength as the angle of incidence increases. This angular dependence may find its application in a photonic crystal superprism.

This work was produced with the assistance of the Australian Research Council (ARC) under the ARC Centres of Excellence Program. The Centre for Ultra-high Bandwidth Devices for Optical Systems is an ARC Centre of Excellence. M. Gu's e-mail address is mgu@swin.edu.au.

References

1. E. Yablonovitch, Phys. Rev. Lett. **58,** 2059 (1987).
2. S. John, Phys. Rev. Lett. **58,** 2486 (1987).
3. K. M. Ho, C. T. Chan, and C. M. Soukoulis, Phys. Rev. Lett. **65,** 3153 (1990).
4. A. Moroz and C. Sommers, J. Phys. Condens. Matter **11,** 997 (1999).
5. H. S. Sözüer, J. W. Haus, and R. Inguva, Phys. Rev. B **45,** 13962 (1992).
6. G. R. Yi and S. M. Yang, J. Opt. Soc. Am. B **18,** 1156 (2001).
7. Z. Y. Li and Z. Q. Zhang, Phys. Rev. B **62,** 1516 (2000).
8. M. M. Sigalas, C. M. Soukoulis, C. T. Chan, R. Biswas, and K. M. Ho, Phys. Rev. B **59,** 12767 (1999).
9. R. C. Schroden, M. Al-Daous, C. F. Blanford, and A. Stein, Chem. Mater. **14,** 3305 (2002).
10. M. E. Turner, T. J. Trentler, and V. L. Colvin, Adv. Mater. **13,** 180 (2001).
11. F. Garcís-Santamaría, C. López, F. Meseguer, F. López-Tejeira, J. Sánchez-Dehesa, and H. T. Miyazak, Appl. Phys. Lett. **79,** 2309 (2001).
12. E. N. Glezer and E. Mazur, Appl. Phys. Lett. **71,** 882 (1997).
13. H.-B. Sun, Y. Xu, S. Matsuo, and H. Misawa, Opt. Rev. **6,** 396 (1999).
14. H.-B. Sun, Y. Xu, S. Juodkazis, K. Sun, M. Watanabe, S. Matsuo, H. Misawa, and J. Nishii, Opt. Lett. **26,** 325 (2001).
15. K. Yamasaki, S. Juodkazis, M. Watanabe, H.-B. Sun, S. Matsuo, and H. Misawa, Appl. Phys. Lett. **76,** 1000 (2000).
16. D. Day and M. Gu, Appl. Phys. Lett. **80,** 2404 (2002).
17. M. J. Ventura, M. Straub, and M. Gu, Appl. Phys. Lett. **82,** 1649 (2003).
18. M. Straub, M. Ventura, and M. Gu, Phys. Rev. Lett. **91,** 043901 (2003).
19. G. Zhou, M. J. Ventura, M. Straub, M. Gu, A. Ono, S. Kawata, X. H. Wang, and Y. Kivshar, Appl. Phys. Lett. **84,** 4415 (2004).
20. D. Day and M. Gu, Appl. Opt. **37,** 6299 (1998).